RESEARCH

Decoupling factor, aerodynamic and canopy conductances of a hedgerow olive orchard under Mediterranean climate

Gianfranco Rana[1] · **Gabriele De Carolis**[1] · **Liliana Gaeta**[1] · **Sergio Ruggieri**[1] · **Rossana M. Ferrara**[1]

Abstract

The degree of coupling between canopy and atmosphere, through the decoupling factor Ω, well describes the behaviour of a crop concerning its water use and carbon dioxide exchange. Super high-density hedgerow olive orchard system is in great expansion all over the world and, since it has a complex field structure in rows of adjacent trees, investigations are necessary to assess the Ω patterns, as well as aerodynamic (g_a) and canopy (g_c) conductances in different water conditions. In this study, in a hedgerow olive orchard (cv. "Arbosana") submitted to full (FI) and regulated deficit irrigation (RDI), cropped under a Mediterranean semi-arid climate (southern Italy), Ω has been determined using g_c, as deduced by inverting the Penman-Monteith equation, and g_a, by upscaling the wind speed measured in a close station to the canopy; the transpiration has been measured by sap flow thermal dissipation method. The results showed that this olive orchard results very well coupled to the atmosphere, in any soil water conditions; Ω is generally very low, being during daytime equal in mean to 0.021 ± 0.003 ms^{-1} and 0.018 ± 0.004 ms^{-1} for RDI and FI, respectively. This condition is linked to g_a and g_c values; in fact, canopy conductance is much smaller than the aerodynamic one in any water and climatic conditions, except when all canopy surfaces are saturated in water. In this latter case, the g_c assumes the highest values due to the contribution of the part of conductance attributable to the structure of the orchard.

1 Introduction

The thermodynamic and aerodynamic relationships between vegetated surfaces and the atmosphere, at different spatial scales from leaves to stand, have been amply investigated in the second half of the twentieth century. Since the introduction of the concept of elastic coupling between canopy and atmosphere, quantified through the *decoupling factor* Ω by McNaughton and Jarvis (1983), canopy transpiration (T) has been effectively characterized by the canopy (g_c) and stomatal (G_s) conductances, both in terms of magnitude and environmental control, especially for tree crops and stands (Wullschleger et al. 2000). When the decoupling factor is high, transpiration is controlled more by incoming radiation and less by changes in stomatal conductance; when it is low, stomal control of transpiration is high and change in

stomal conductance results in a corresponding change in transpiration.

Insights into the degree of coupling between vegetation and the atmosphere permit to investigate the behaviour of a species in term of its water use, as well as the exchange of carbon dioxide between the canopy and the atmosphere (de Kauwe et al. 2017).

The degree of coupling depends strongly on the aerodynamic characteristics of the vegetated surface (Jarvis and McNaughton 1986; McNaughton and Jarvis 1991), such as surface roughness, foliage clumping, leaves shape and density, canopy density, plant height, and training system. High canopy and species with small leaves are expected to be more strongly coupled to the atmosphere than low canopy and species with large leaves: this is because high plants have high surface roughness and thus high aerodynamic conductance which directly links the transpiration surface to the above atmospheric environment. At a continuous scale of plant height and surface roughness, there are a number of intermediate possibilities. Ω is also dependent on air temperature, through the effect of temperature on the slope of the vapor pressure-temperature

✉ Gianfranco Rana
gianfranco.rana@crea.gov.it

1 Council for Agricultural Research and Economics, Agriculture and Environment Research Centre (CREA-AA), Bari, Italy

relationship, and also showed a fourfold variation in its diurnal pattern in tree crops (Köstner et al. 1992).

Actual transpiration at the canopy scale results from the integration of instantaneous processes at the leaf level. However, investigations at the canopy level can be faced by considering the vegetated surface as a single entity characterized by (i) a bulk canopy conductance (g_c) for water transfer and (ii) an aerodynamic conductance (g_a) for the transfer of momentum and other scalars between the canopy and the atmosphere; thus, the canopy can be considered as a single "big-leaf" (Monteith and Unsworth, 1990).

In the relationship between vegetated surface and atmosphere, G_s and g_c have different boundary conditions because they express exchange processes at different spatial scales. In the big-leaf approach net radiation (R_n) is assumed to be received in the same environment by an identical surface at air temperature processes (Martin 1989; Monteith and Unsworth, 1990). Furthermore, the relation between canopy as a whole and air vapour pressure deficit (D) is different from the relation between the leaf and D in the local leaf boundary layer (McNaughton and Jarvis 1991; Baldocchi et al. 1991; Katerji and Rana 2011). Therefore, precautions about where thermodynamic measurements are realized and how the canopy aerodynamic characteristics are determined must be taken when the coupling with atmosphere is studied at canopy scale where, usually, g_c is derived by inverting the model to estimate the transpiration (Zhang et al. 2016; De Kauwe et al. 2017). The Penman-Monteith model (Monteith 1965) or simplified versions of it (Köstner et al. 1992) are typically used for these types of investigations.

While many studies on the decoupling factor deal with forest and woody species, the studies on fruit trees are relatively uncommon (see de Kauwe et al. 2017 for a review).

Although, the decoupling factor can be considered as a powerful sensitivity parameter to explore the relationship between transpiration and stomatal closure (Spinelli et al. 2018), the literature reported few studies about Ω in fruit crops during the growth season. Forster et al. (2022) found that along the growth season Ω varied in the range 0.55–0.65 and 0.50–0.55 for apple and pear, respectively, the plants` height was around 5 m for both crops. Marin et al. (2016) gave for Ω a mean value of 0.1 for a citrus orchard of 4 m height, without any indication on the dynamics. Spinelli et al. (2018) give a seasonal dynamic of Ω in the range 0.2–1.0 for an almond orchard following the crop water conditions. Except for the latter study, where measurements were carried out in the centre of the plot by the eddy covariance technique (Lee et al. 2004), the measurements of the weather variables, useful for the application of the used models, were carried out in stations more or less far from the canopy under study, without any type of correction or upscaling.

Since the last few years of the last past century, olive cultivation has intensified considerably, with super high density (SHD) cultivation systems being widespread and growing rapidly in the Mediterranean region (Godini et al. 2011). These new fully mechanized olive groves, known as "hedgerow orchards", are characterised by a density over 1,200 trees per hectare and by the continuous fruit harvesting (Vivaldi et al. 2015). In view of the increasing drought conditions in Mediterranean regions (Katerji et al. 2017), several studies (Iniesta et al. 2009; Fernández et al. 2013; Rosecrance et al. 2015) suggest regulated deficit irrigation (RDI) as a suitable strategy in SHD olive orchards to reduce the typical excessive vigour of the species, by limiting soil water availability.

Tognetti et al. (2009) analysed the Ω values of a standard plantation of 15-year-old olive trees cultivated in the Mediterranean region under different water conditions. They found that Ω was relatively low in a dry summer, implicating a strong control of transpiration by stomatal regulation, with the water-stressed canopy more coupled to the atmosphere than the well-watered one. Conversely, in a wet summer, Ω was quite high and the transpiration becomes increasingly dependent on the R_n received and less dependent on D. Although in this last case it seems that water vapour exchange was mainly controlled by leaf conductance, evaporative demand, solar radiation, soil moisture and the functioning of the canopy and root systems had varying complex influences on canopy-scale stomatal control of water, needing further mid-term investigations under contrasting weather conditions (Tognetti et al. 2009; de Kauwe et al. 2017; Chebbi et al. 2018).

Hedgerow tree orchards have peculiar aerodynamic characteristics, because the regular arrangement of close adjacent trees, in rows separated by soil strips, makes the roughness highly dependent on the angle between the wind direction and the orientation of rows (Alfieri et al. 2019). Zeng and Wang (2007) found that neglecting factors beyond canopy height and plantation structure can affect surface roughness by introducing significant errors of up to 50%. Maurer et al. (2013, 2015) have shown that errors in roughness length and zero-plane displacement height can result in significant errors in modelled fluxes and related variables. Therefore, the impacts of both aerodynamic characteristics and aerodynamic conductance on Ω need to be deeply analysed for assessing the control of the environment on the water canopy behaviour in different crop water conditions, especially if the plantation has such an in-row hedgerow structure.

Tree structure (Daudet et al. 1999) and, more extensively, canopy structure (Baldocchi et al. 1991; Spinelli et al. 2018) are linked to the degree of coupling between the crop and the atmosphere. Kjelgaard and Stockle (2001), on the base of the studies by Perrier (1975a, 1975b), used the concept of an additional non-stomatal "excess conductance", together with

the canopy conductance, to determine the total conductance to water vapor transport from surface toward atmosphere. The existence of such a structural conductance was since measured canopy conductance underestimated the scaled-up stomatal conductance (Kjelgaard and Stockle 2001). Unfortunately, at our best knowledge, the studies on the estimation of this structural conductance are rare, also for crop having complex aerodynamic structure as hedgerow canopies, because it can be obtained only when all surfaces are saturated, and the canopy conductance is maximum.

The general objective of this mid–term study was to investigate and analyse the relationships among decoupling factor, aerodynamic and canopy conductances of olive trees (cv. *Arbosana*) grown in a hedgerow orchard submitted to full irrigation (FI) versus regulated deficit irrigation regime (RDI). Specific aims are: (i) to establish which environmental factors affect the decoupling coefficient; (ii) how environmental and physiological factors affect the decoupling coefficient; (iii) if and how the structure of the plot can affect the degree of decoupling between vegetated surface and atmosphere; (iv) which precautions should be adopted to have correct estimation of decoupling factors. Measurements were carried out in the hottest months of three growing seasons (2019-2021) in a Mediterranean environment (southern Italy), characterised by contrasting weather conditions.

2 Material and methods

2.1 Theoretical framework

The transpiration is a process occurring at leaf level. However, "the single-layer model (…) is adequate to illustrate the nature of the meteorological feedback processes which operate in much the way we describe, although they must be represented in a more complex fashion in more complex models of canopy processes" (McNaughton and Jarvis 1991). Hence, the theoretical upscaling framework of transpiration (T) from leaves to canopy is left to the cited literature: here we adopt the "big-leaf" approach to estimate the hedgerow olive orchard transpiration under the following form:

$$\lambda T = \frac{\varepsilon A + \varrho c_p D g_a / \gamma}{\varepsilon + 1 + g_a / g_c} \tag{1}$$

where λ is the latent heat of vaporization of water (J kg^{-1}), A is the available energy (R_n-G), with R_n the net all-wave radiation above the stand (J m^{-2} s^{-1}), G the heat flux to soils (J m^{-2} s^{-1}), ρ the mean air density (kg m^{-3}), c_p the specific heat of air at constant pressure (J kg^{-1} K^{-1}), D the atmospheric vapour pressure deficit (kPa), $\varepsilon = \Delta/\gamma$ with Δ the rate of change of saturation water vapor pressure with temperature (kPa K^{-1}) and γ the psychrometric constant (kPa

K^{-1}), g_a the aerodynamic conductance (m s^{-1}) and g_c the canopy conductance (m s^{-1}). Since the olive orchard was drip irrigated, the evaporation component is low than 10% of evapotranspiration (Bonachela et al. 2001; Egea et al. 2016) and was here neglected.

In Eq. (1), it is supposed (Monteith 1965) that the energy conservation principle is applied to the zero-plane displacement (the height of the plane, d (m), considered as origin, $z = 0$, for the coordinate system in which the model is formulated or, in other words, the level of the base of the roughness elements). Thus, the energy balance is a boundary condition applied on a plane $z(0)$ where the energy is entirely available, i.e., $z(0) = d+z_0$, with z_0 the roughness length for momentum transfer.

The model expressed by Eq. (1) introduces two conductances expressing the transport of water from the canopy to the atmosphere: (i) the canopy conductance, g_c, which describes the diffusion of vapour due to stomatal regulation of the canopy thought as a big leaf; (ii) the aerodynamic conductance, g_a, between the zero-plane displacement and a reference plane over the canopy, which accounts for the convective transport of vapour toward the atmosphere.

In this study, since the evaporative surface is heterogeneous and the architecture of such a hedgerow canopy is complex and has impacts on the convective transport of water vapour, we make the following hypothesis:

(i) the canopy is a semi-porous medium where the mechanism of vapor diffusion is strongly influenced by both the architecture of the canopy and the stomatal regulation (Perrier 1975a; Daudet et al. 1999, among others);

(ii) the energy conservation boundary condition is applied to the top of the canopy, so that

(iii) the aerodynamic resistance is experimented between this plane and the reference surface;

(iv) the canopy conductance indicated as diffusion canopy conductance, g_{cd}, (Perrier 1975b; Katerji and Rana 2011), can be written as:

$$\frac{1}{g_{cd}} = r_c + r_0 \tag{2}$$

with r_0 resistance depending on the canopy structure (Appendix 5.) and r_c resistance depending on the mean stomatal regulation of leaves.

Under these hypotheses, introducing Eq. (2) in Eq. (1), the canopy conductance of Eq. (1) becomes "g_{cd}" and maintains the same meaning of the big leaf approach by Monteith (1965), while the aerodynamic conductance is expressed as (Perrier 1975a; Rana et al. 1994; Katerji and Rana 2011)

$$g_a = \frac{k^2 u(z)}{\ln\left(\frac{z-d}{z_0}\right)\ln\left(\frac{z-d}{h_c-d}\right)} \tag{3}$$

z (m) is the height of the reference plane, d (m) is the zero-plane displacement height of the measurement surface, z_0 (m) is the roughness length for momentum transfer, h_c (m) is the mean crop height, k (0.4) is the von Karman constant; $u(z)$ (m s^{-1}) is the wind speed at the reference height above the canopy. The above relationship is valid in neutral atmospheric conditions, and it assumes a logarithmic profile of wind speed and air temperature in the convective boundary layer and on the mixing length turbulent model.

Under the above assumptions, the actual transpiration for the hedgerow olive orchard can be written as

$$\lambda T = \frac{\varepsilon A}{\varepsilon + 1 + g_a/g_{cd}} + \frac{\rho c_p D g_a/\gamma}{\varepsilon + 1 + g_a/g_{cd}} \tag{4}$$

Two terms appear in this expression: the first one is the "radiative term", representing the contribution of the radiative energy to T, the second one, called "convective term", is due to both the natural and forced convection in the low atmosphere above the canopy (Monteith 1965; Jarvis and McNaughton 1986; Rana et al. 1994).

To establish the boundary values of g_a, the limits of λT for $g_a \to \infty$ and $g_a \to 0$ must be calculated for the full and null coupling between canopy and atmosphere, as (Jarvis and McNaughton 1986):

$$\lim_{g_a \to 0}(\lambda T) = \frac{\varepsilon}{\varepsilon + 1} A = \lambda T_{eq} \tag{5a}$$

$$\lim_{g_a \to \infty}(\lambda T) = \frac{\rho c_p}{\gamma} D g_{cd} = \lambda T_{imp} \tag{5b}$$

The term (5a) is known as "equilibrium transpiration", because the canopy is completely decoupled from the atmosphere and the transpiration is addressed only by the available energy at the canopy reference surface; the term (5b) is known as "imposed transpiration", because the canopy is fully connected to the atmosphere and the transpiration is addressed by the stomatal regulation at a given thermodynamic condition of air expressed by vapour pressure deficit D. Between these two boundary values for g_a, a decoupled factor Ω, having values in the range $0 – 1$, can be defined (Jarvis and McNaughton 1986) to take into account all actual possibilities, as:

$$\Omega = \frac{\varepsilon + 1}{\varepsilon + 1 + g_a/g_{cd}} \tag{6}$$

therefore, the transpiration can be determined in "elastic" way as:

$$\lambda T = \Omega \lambda T_{eq} + (1 - \Omega)\lambda T_{imp} \tag{7}$$

Figure 1 (adapted by Rana et al. 1994) reports some examples of relationship between λT and g_{cd} for some values of wind speed v, at given thermodynamic condition of the atmosphere for a typical clear spring morning in Mediterranean region. A particular value of g_{cd}, known as "critical conductance", g^* (firstly described by Daudet and Perrier 1968, in an unfamiliar and rarely cited study of several decades ago) divides the graph in two zones, A and B; in the zone A ($g_{cd} > g^*$) the transpiration is an increasing function of the wind speed; in the zone B ($g_{cd} < g^*$) the transpiration decreases with the wind speed; the latter phenomenon is less evident but has strong impacts on the coupling of tree orchards (Daudet et al. 1999). To give an expression to the critical conductance g^* it is necessary to look for the characteristic value of g_{cd} that annuls the derivative $\partial \lambda T/\partial g_a$ (Rana et al. 1994, 1997) i.e.:

$$g^* = \frac{\Delta A}{(\varepsilon + 1)D\rho c_p} \tag{8}$$

It is useful to underline the dependence of g^* on climatological factors only and that it is quasi-linearly correlated to the Monteith (1986) "climatic or isothermal conductance"

$$g_i = \frac{\gamma A}{D\varrho c_p} \tag{9}$$

If we substitute the expression (8) into (4), it is possible to write the decoupling framework of λT under the form:

$$\frac{\lambda T}{A} = \Omega \frac{\varepsilon}{\varepsilon + 1} + (1 - \Omega)\frac{\varepsilon}{\varepsilon + 1}\frac{g_{cd}}{g^*} \tag{10}$$

The above expression provides a clear interpretation for the coupling process between canopy and atmosphere (Jarvis and McNaughton 1986):

1. When $\Omega = 1$ (canopy isolated by atmosphere), the transpiration is an almost fixed constant fraction of available energy (Priestley and Taylor 1972) at equilibrium between the crop in given water conditions and the atmosphere.
2. When $\Omega = 0$ (canopy fully coupled to atmosphere), the conditions are imposed by the atmosphere and the crop proceeds at transpiration rates depending on the weather (g^*) and is effectively controlled by the stomatal regulation at instantaneous time scale (g_{cd}).

2.2 The aerodynamic conductance

The value of Ω may be submitted to wide variations depending on the aerodynamic roughness of the transpiring unit (see Eqs. 3 and 6). Furthermore, correct estimations of the aerodynamic conductance, which determine the degree of coupling, are difficult to obtain because wind speed is usually measured at short distance from the

Fig. 1 Variation of the transpiration versus the diffusion canopy conductance and the wind speed (adapted by Rana et al. 1994)
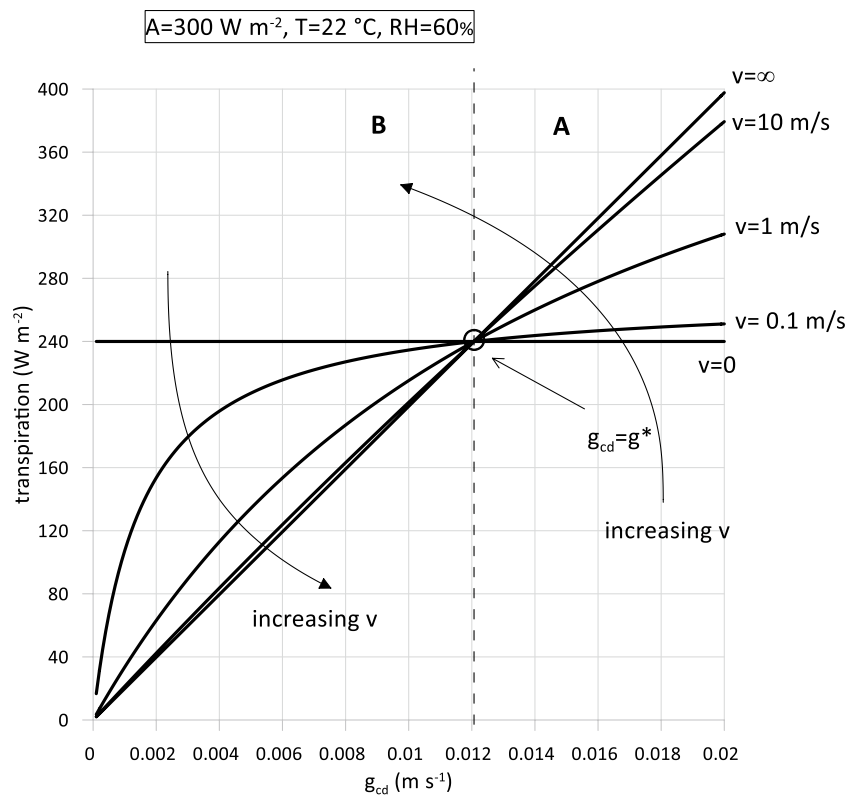
surface, whereas gradients of temperature and humidity often persist for large distance above the reference level; McNaughton and Jarvis (1983) estimated that about one-third of the conductance across the surface layer is located above the usual instrument height.

Therefore, the aerodynamic characteristics at the interface canopy-atmosphere inside the fully developed boundary layer, through the roughness and zero plane-displacement lengths and the wind speed at the reference height, must be accurately determined to have correct Ω values.

~~Here,~~ Since the canopy structure of the olive stand is in rows of closed adjacent trees, the roughness length of momentum transfer was calculated as suggested by Alfieri et al. (2019), who identified a sigmoidal relationship between z_0 and wind direction:

$$z_0 = \xi_{min} + \frac{\xi_{max} - \xi_{min}}{1 + \exp\left[-\beta\left(\omega - \omega_0\right)\right]} \quad (11)$$

where ω is the relative wind direction, defined as 0° when the wind direction is parallel to the row direction, i.e., north to south, and 90° when the wind direction is perpendicular to the row. In Eq. (11) the fitting parameters of the sigmoid function ($\xi_{min}=0.1642$, $\xi_{max}=0.3107$, $\beta=0.1270$, $\omega_0=24.52$) were found by Alfieri et al. (2019) in a vineyard crop; here

the same values were used for this olive orchard after an experimental test (see Supplementary material 1). Anyway, after a sensitivity analysis on z_0, we found that a variation of $\pm10\%$ in the fitting parameters brings to an uncertainty of $\pm6\%$ in mean on z_0. The zero-plane displacement height was set $d = 0.67\ h_c$.

Since Ω is referred to the canopy site, and the weather variables were here measured in a separate meteorological station (see next section), Rana and Katerji (2009) were followed to upscale variables from the station to the canopy (Supplementary material 1).

2.3 The canopy stomatal conductance

Although here the analysis was made at the canopy level, and the canopy conductance was derived by the inversion of the Penman-Monteith model (Eq. 1), and conscious that the canopy conductance is not a purely physiological variable (i.a., Rochette et al. 1991), an investigation by using independent measurements at leaf scale can support the correctness of the found g_{cd}, at least regarding the order of magnitude. The theoretical development of the leaf stomatal conductance scaling up to the canopy is left to the extensive literature on the subject (see for example the physical approach proposed by Baldocchi et al. 1991, among many

others); here we estimate a mean stomatal canopy conductance (g_{sc}, m s^{-1}) as (Szeicz and Long 1969):

$$g_{sc} = \frac{RT_l}{P_a}\overline{G_s}LAI \tag{12}$$

with $\overline{G_s}$ (mol m^{-2} s^{-1}) the mean conductance measured at leaf level, LAI leaf area index, R (8.314 J mol^{-1} K^{-1}) the gas constant, T_l (K) the leaf temperature and P_a the atmospheric pressure (set at standard value equal to 101325 Pa). The LAI values were estimated as detailed in Supplementary material 2.

2.4 The site, the crop, and ancillary measurements

The study was realized in three years (2019, 2020 and 2021) focusing on the most evaporative demanding periods in the site (Katerji et al. 2017), i.e. from 1 July to 31 August. The olive orchard (cv. *Arbosana*) is located at the University of Bari experimental farm at Valenzano, southern Italy (41° 01' N; 16° 45' E; 110 m a.s.l.), on a sandy clay soil (sand, 630 g kg^{-1}; silt, 160 g kg^{-1}; clay, 210 g kg^{-1}) classified as a Typic Haploxeralf (USDA) or Chromi-Cutanic Luvisol (FAO). The site is characterised by typical Mediterranean climate with a long-term average (1988-2018) annual rainfall of 560 mm, two third concentrated from autumn to winter, and a long-term average annual temperature of 15.6 °C. The olive grove has been planted in early summer 2006; the self-rooted trees were trained according to the central leader system and spaced 4.0 m × 1.5 m (1,667 trees ha^{-1}) with a North–South rows orientation, according to the SHD cropping system. Trees were 1.75±0.46 m high. Routine cultural nutrition, soil management, pests and diseases control practices were set up as described by Camposeo and Godini (2010). Lots of 180 m^2 surface, 60 m apart, with 35 trees in each one, were submitted to two irrigation regimes: full irrigated (FI) versus regulated deficit irrigation (RDI), the last applicated throughout the pit hardening phase, when the tree is least sensitive to water deficit; during this phenological phase, irrigation was interrupted for about one month (19/07-20/08/2019; 15/07-18/08/2020; 14/7-14/08/2021). Irrigation was scheduled following the evapotranspiration method, by restoring 100% of crop evapotranspiration lost in each irrigation interval, as recommended by the FAO56 guideline. The plots were irrigated by a dripline equipped with 2.5 L h^{-1} emitters, 0.6 m apart.

Air temperature (T_{air}, °C) and vapour pressure deficit (D, kPa) through air relative humidity, global radiation (R_g, MJ m^{-2} s^{-1}) and precipitation (P, mm), wind speed (u, ms^{-1}) and wind direction (degree) were collected at a standard agrometeorological station 120 m far from the experimental field.

R_n and G, both in Wm^{-2}, was calculated as follows (Rana and Katerji 2009, among others):

$$Rn = (1-\alpha)R_g - \sigma\left(\frac{T_{max}^4 + T_{min}^4}{2}\right)(0.34 - 0.15\sqrt{e_a})\left(1.35\frac{R_g}{R_{g0}} - 0.35\right) \tag{13}$$

where α albedo of the crop directly determined on the orchard as mean of hourly daytime values (0.27) from January to December 2021; T_{max} and T_{min} (K) are maximal and minimal air temperatures; e_a (kPa) is the actual vapour pressure; and R_{g0} (MJ m^{-2}) is the calculated clear-sky radiation. After a local calibration of twelve months (January-December 2021), G was considered as a constant at daily scale and equal to 0.09 R_n.

The degree of drought for each year under investigation was evaluated by the standard precipitation index (SPI, Naresh Kumar et al. 2009).

The Canopy conductance g_{cd} to calculate Ω (Eq. 6) was obtained by inverting Eq. (1)

$$g_{cd} = \frac{\lambda T g_a}{\varepsilon A + \varrho c_p D g_a/\gamma + (\varepsilon + 1)\lambda T} \tag{14}$$

Here actual transpiration was measured by sap flow thermal dissipation method (TDM, Granier 1985, 1987). λT was determined by the sap flow density, J_{s0} (g m^{-2} s^{-1}) measured in a set of selected plants. Specific calibration of TDM, corrections induced by the wounds and other errors (azimuth and trunk gradient) were carried out as described in Supplementary material 3.

Soil water content in volume (θ, m^3 m^{-3}) was measured by capacitive probes (5TM, Decagon Devices Inc., USA). For each treatment, three points were monitored following the protocol described in Campi et al. (2020). At each point, two capacitive probes were installed horizontally into the soil profile and transversely to the row, at −0.12 and −0.37 m from the soil surface to intercept the dynamics of θ below the dripping lines. One set of probes was installed between the tree rows. All sensors were connected to data-loggers (Tecno.el srl, Italy); integrated soil water content daily was determined for the soil profile (0.5 m) by integrating the three values measured at each depth, since each probe was supposed to detect the water content in a 0.25-m soil layer (Campi et al. 2019). θ measurements from the three points were pooled to obtain a single average value for each treatment.

Soil water availability was described through the relative extractable water (REW, unitless) calculated using the average soil water content across positions around the tree and soil layers (Granier 1987; Tognetti et al. 2009):

$$REW = \frac{\theta - \theta_{min}}{\theta_{max} - \theta_{min}} \tag{15}$$
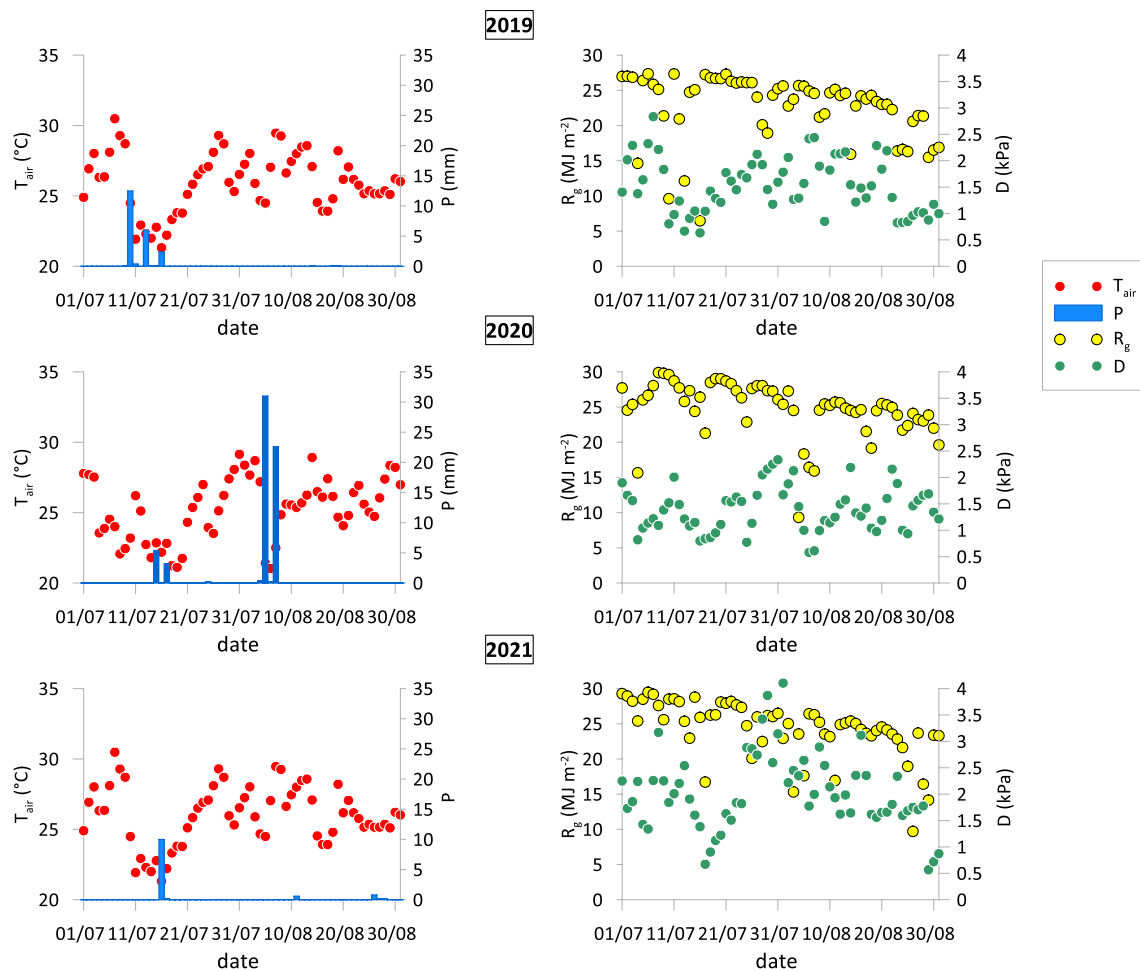
Fig. 2 Daily patterns of air temperature (T_{air}), precipitation (P), vapour pressure deficit (D) and global radiation (R_g) in the three experimental periods

where θ is the actual soil water content in the root zone, θ_{min} the minimum soil water content observed during the experiment, and θ_{max} is the maximum soil water content in the area (e.g., at field capacity).

Stomatal conductance (G_s, mol_{H2O} m^{-2} s^{-1}) was measured (2, 23, 31 July and 29 August 2019) on two healthy well light-exposed leaf per tree (on the West and East side) selected in the middle part of the canopy, by using a portable open gas-exchange system, fitted with a LED light source (LI-6400XT, LI-COR, Lincoln, NE, USA). At each measurement and canopy side, light intensity was maintained constant across the two treatments setting the LED light source at the natural irradiance detected near the leaf. For each treatment, G_s measurements were performed in the three plants where transpiration was measured by TDM and other two trees similar for dimension, vigour and health state, chosen in correspondence with the soil moisture probes. The data were subjected to one-way ANOVA using SAS/STAT 9.2 software package (SAS/STAT, 2010).

3 Results and discussion

3.1 Weather, soil water and aerodynamic characteristics of the orchard

The time evolution of main meteorological parameters (daily values of T_{air}, D, R_g and P) in the experimental periods are shown in Fig. 2. The three periods were characterized by very different weathers, including the extreme water scarcity conditions during the 2019 and 2021 drought summers, and the exceptionally rainy summer in 2020 characterized by few events and high rain intensity. In few minutes, 31 and 23 mm of rain fell on 5th and 7th August 2020, respectively. The much-contrasted weather of the three years confirms the great variability following the climate change, in terms both of temperature and rain of the last years in this Mediterranean area (Rana et al. 2016; Katerji et al. 2017). The yearly mean air temperature was 18.1, 16.4 and 17.0 °C in 2019, 2020 and 2021, respectively, being always warmer

Fig. 3 The relative extractable water (REW, unitless) daily trend in the three experimental periods in both Full Irrigation (FI) and Regulated Deficit Irrigation (RDI) treatments; irrigation and precipitations are also graphed. The horizontal dashed red line at REW = 0.4 indicates threshold for water stress by literature
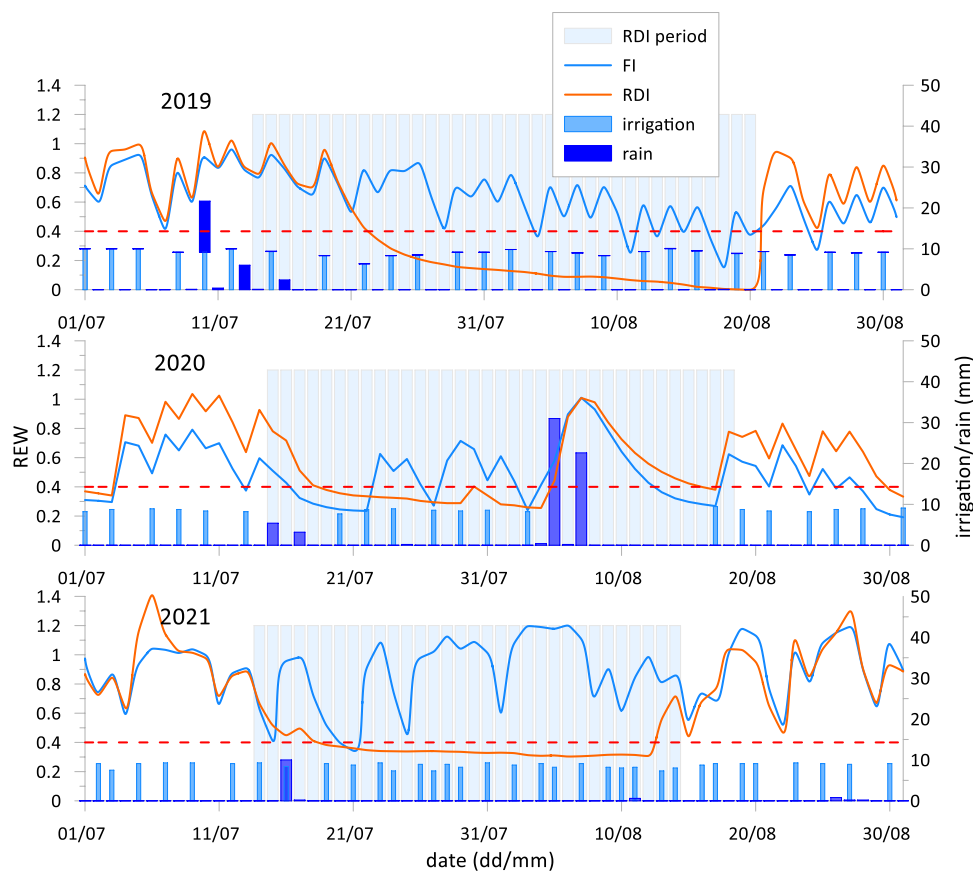
than in the past (15.6 °C). Furthermore, an intense heat wave crossed the experimental period in 2021, between end July and beginning of August, when irrigation was withheld in the RDI plot. Mean air temperature attained 34 °C and peaks of 42 °C were observed during daytime. Moreover, in these periods D reached high values, unusual for the region. The SPI was equal to -1.61, +0.96 and -1.45 for whole years 2019, 2020 and 2021, respectively, indicating that 2020 was extremely wet, while 2019 and 2021 were very dry.

The *REW* trends at daily scale in the three growing seasons are shown in Fig. 3, together with irrigations and precipitations, for the FI and RDI treatments. In both treatments the *REW* increased immediately after any water supply or rainfall and, conversely, decreased quite steeply follow plants' transpiration. For RDI treatment the soil water recovery after the irrigation interruption period happened in the same day of watering accordingly with Fernández (2014).

According to irrigation scheduling, before and after irrigation interruption period, water supply results the same for FI and for RDI. In these periods, FI and RDI trends are almost superimposable. Small differences are due to the different total water availability in the two plots (0.105 and 0.122 m³ m⁻³ for FI and RDI, respectively) and to different minimum value of SWC in the two soils (0.144 and 0.151 m³ m⁻³ for FI and RDI, respectively). In the FI treatment,

REW values did not fallow below 0.3, reaching values near or greater than 1 when soil water conditions were at field capacity or above it, just after frequent irrigations and/or heavy precipitations. In the RDI treatment, *REW* values was below 0.4 for most of the irrigation season, indicating soil water conditions quite far from the field capacity, except in short periods just after frequent irrigations and/or heavy precipitations. In the RDI treatment, *REW* values decreased when irrigation supply was reduced, in any growth season. The minimum *REW* values in RDI treatment were 0.0, 0.1 and 0.15 in the first, second and third season, respectively.

Several studies indicated that plants are exposed to increasing water stress when the REW value falls below 0.4, mainly for woody species under arid and semiarid Mediterranean conditions (Bréda et al. 1995; Fernández et al. 1997; Grossiord et al. 2015). In the present study, focusing on the RDI period, *REW* values fell below 0.4 for 7 and 29 days in FI and RDI treatments, respectively in the first season; 13 and 18 days in the second season; 2 and 25 days in the third season.

Figure 4 shows the distribution of z_0 values at hourly scale, as number of values in a class of 0.01 m, calculated using Eq. (11), are shown for all seasons. z_0 ranged between 0.17 m and 0.31 m, having a mean value of 0.25 m; the highest values correspond to winds in the direction East-West,
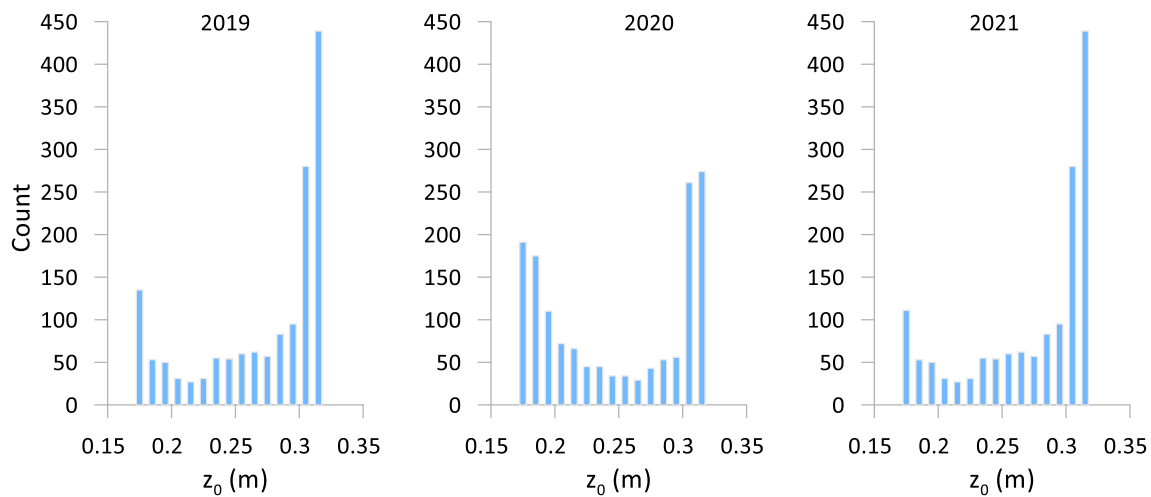
Fig. 4 Distribution of roughness height (z_0) values at hourly scale in the three investigated experimental periods; count is the number of values in a class (bin=0.01 m)

perpendicular to the tree rows. If a fixed value of z_0 is used, for example z_0=$0.1h_c$, the underestimation on z_0 was about −20% (data not shown), but of course this depends strongly on the wind direction. In fact, when the wind flows perpendicularly to the rows (East–West) the underestimation is until −47%, while when the wind flow parallelly to the tree rows (North–South) the underestimation is much lower (until −7%); in our site, the predominant winds come from North and South (63% of runs).

3.2 The canopy conductance and the decoupling factor

Before the presentation of the decoupling factor trend for the two treatments FI and RDI, it is worth to evaluate all terms involved in the transpiration process for this hedgerow olive orchards: i.e., the aerodynamic, the critical and the diffusion canopy conductances (see Eqs. 6 and 10).

The aerodynamic conductance values are shown in Fig. 5 in function of the wind direction for the three seasons. The values calculated using the corrected upscaled wind speed (see Eq. 1.1 in Supplementary material 1) are much lower than the values of g_a calculated using the wind speed as measured by the nearby weather station: this last g_a overestimates of about 55% the actual g_a value above the orchard. The highest g_a values were found when the wind flowed from East, in correspondence of the highest values of the roughness length. The g_a mean values in the three seasons were equal to 0.10, 0.11 and 0.12 m s^{-1} for the years 2019, 2020 and 2021, respectively.

The hourly trends during the day of aerodynamic, critical and canopy conductances, are shown in Fig. 6, for both treatments; the results are divided in three periods: the first one before the withholding irrigation for RDI, the second one

corresponding to the withholding irrigation and the third one after it. Note the logarithmic scale of Y axe, for focusing the difference on the order magnitude among conductances. The aerodynamic canopy conductance, g_a, is in any case much greater than the other conductances, having almost the same trends for all periods and seasons. In fact, it always follows a bell shape (masked of course by the logarithmic scale) with maximum values in early afternoon.

The trends of the canopy conductances g_{cdFI} and g_{cdRDI} for FI and RDI treatments, respectively, follow complex paths along the day.

After an ANOVA analysis on mean daily values, the most significant differences between the diffusive conductance in the two treatments were detected during night-time. Nocturnal stomatal conductance was observed in a wide range of species and ecosystems and, although different environmental, functional and physiological factors were individuated to explain the nocturnal transpiration (see the review by Resco de Dios et al. 2019 for example), for olive trees the causes and the consequences of the plant nocturnal response, as well as the costs and benefits of nocturnal transpiration remain still unclear (Brito et al. 2018). During night, we found significantly ($P<0.01$) higher values of g_{cdFI} than g_{cdRDI}, in the second and third seasons, comparable to results found by López-Bernal et al. (2010) for an olive orchard in Spain. This topic would merit to be further investigated, although it is outside the scope of the present study.

Focusing attention on mean daily values ($R_g > 20$ Wm^{-2}), the canopy conductance values in the withholding irrigation period were significantly higher ($P<0.01$) in FI treatment than RDI, in the first and third growth season. In the second season 2020, the canopy conductance values of both treatments were not significantly different: in this case the pattern could be explained by the huge

Fig. 5 Aerodynamic conductance (g_a) values in function of the wind direction for the three analysed experimental periods analysed in the text. Solid lines represent g_a calculated with upscaled wind speed (see text)
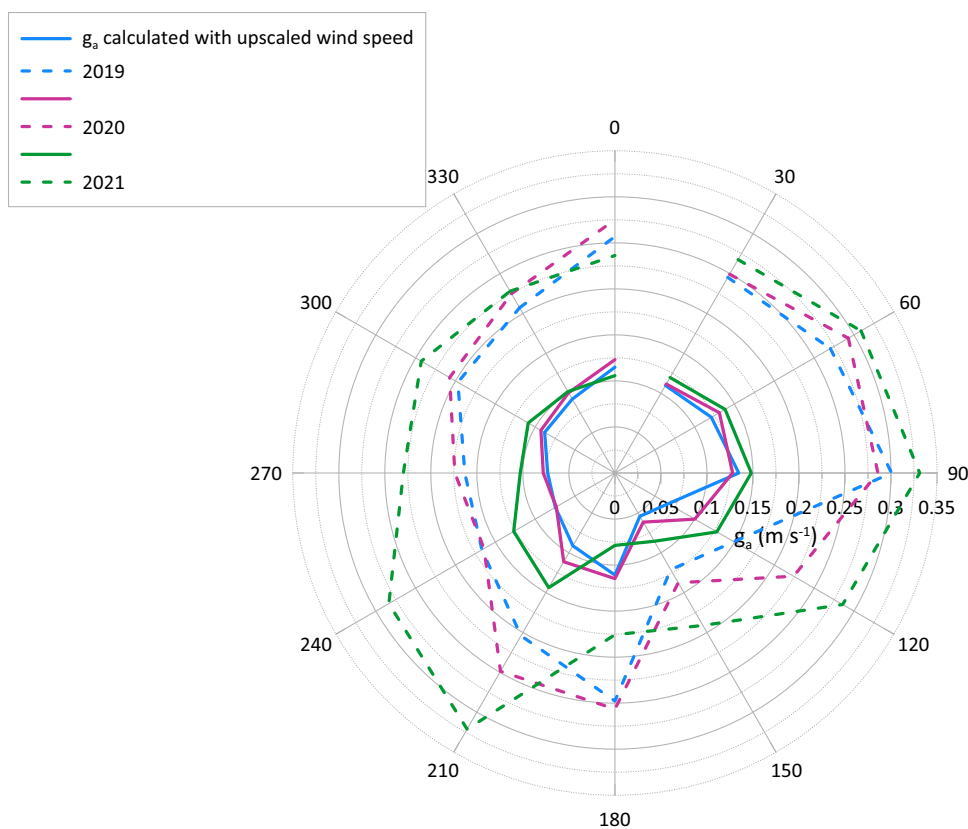

rain attenuating the differentiation between irrigation treatments. Furthermore, g_{cRDI} was significantly higher ($P<0.01$) than g_{cFI} in the second, 2020, and third, 2021, growth seasons during the first irrigation period, and in the third season during the second irrigation period; the canopy conductance values were not significantly different otherwise. These differences could be explained by the difference water contents due to the different total water availability in the soils of the two treatments, as above discussed (see Fig. 3).

In each case, canopy conductance values for both treatments increase in the early morning, followed by a decrease in the hottest hours and a further increase in the early afternoon.

The critical conductance g^* followed trends with intermediate values between g_a and g_{cd}, always having a well-defined bell shape during the day, when the solar radiation is positive. The values of g^* are always greater than g_{cd}, except in a few cases around the sunset or sundown; therefore, for this specific hedgerow olive orchard we are in the zone B of the graph in Fig. 1, which theorizes that transpiration decreases with increasing of wind speed. To verify and represent this behaviour, in Fig. 7, the relationships between transpiration (in energy terms) and wind speed are shown for different specific meteorological conditions for both treatments, at hourly scale; for clarity all available values were binned (bin equal
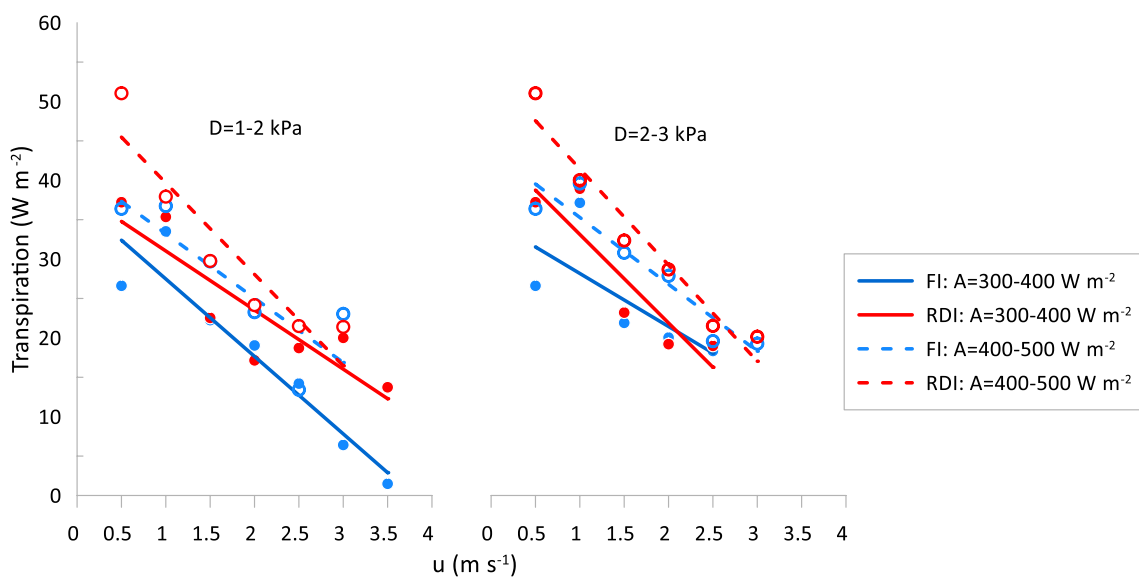
to 0.5 m s^{-1}) and the standard deviations are not indicated. The figure underlines that, at specific given meteorological condition expressed by D and A, the transpiration decreases with the increase of the wind speed, which is a counterintuitive fact rarely illustrated with experimental data (Daudet et al. 1999). This is due, of course, to very lower values of the canopy conductance with respect to the aerodynamic conductance, which means that the canopy is completely coupled to the atmosphere. In this case the transpiration is very little affected by the aerodynamic conductance and completely addressed by the canopy behaviour in terms of stomatal regulation, which in turn depends on the D and, much less, on the available energy.

To dispel any doubts about the orders of magnitude found in the estimated canopy conductance, and to avoid any artifact introduced from the Penman-Monteith inversion mathematical procedure, a comparison between g_{cd} and the canopy stomatal conductance, g_{sc}, directly deduced by measurements at leaves scale and LAI (Eq. 12) was realized, for several days of 2019, when hourly measurements of $\overline{G_s}$ were carried out along daytime. Figure 8 illustrates the hourly patterns of diffuse canopy and stomatal conductances calculated as mean of available values, for both FI and RDI treatments. From the comparison it is clear that the patterns have similar trend for both variables in the part of day considered; however,
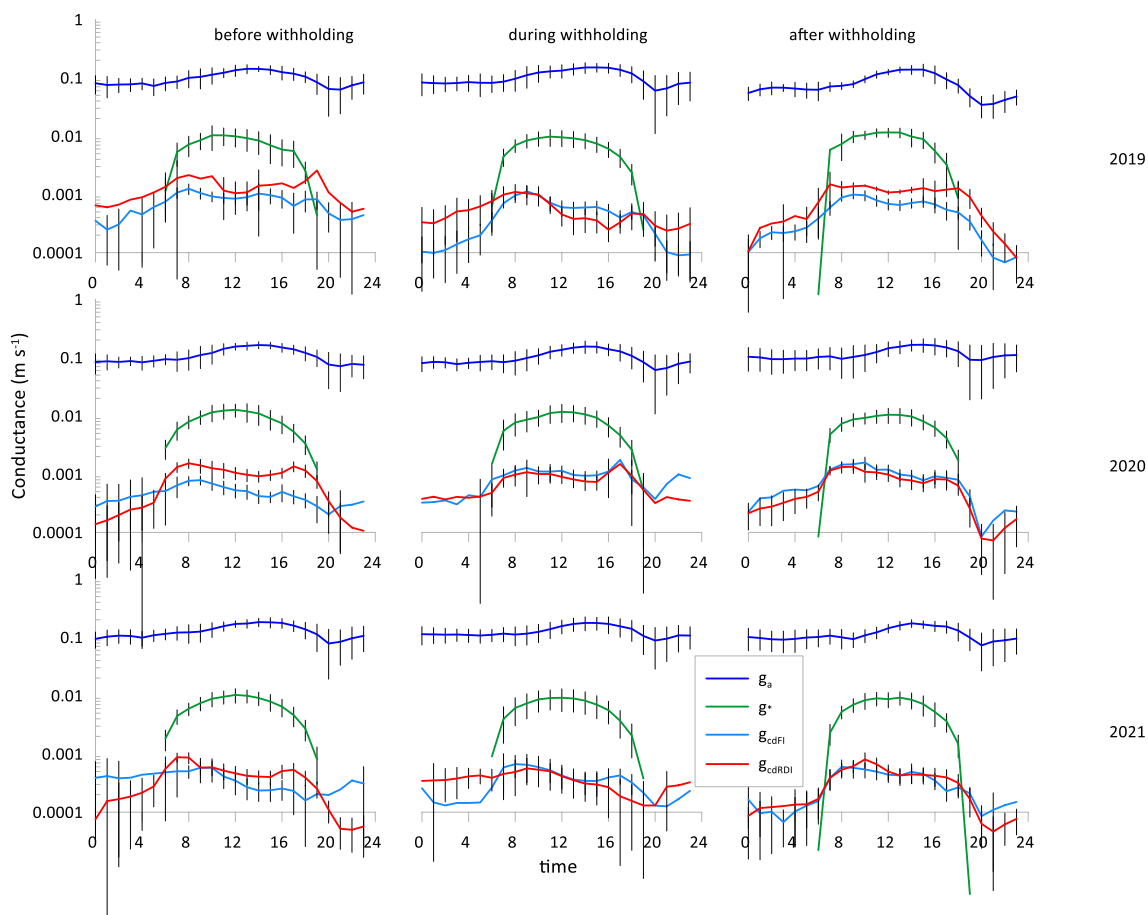
Fig. 6 Hourly trends during the day of aerodynamic (g_a), critical (g^*) and diffuse canopy conductances (g_{cd}), for Full Irrigated (FI) and Regulated Deficit Irrigation (RDI) treatments, before the withholding irrigation for RDI, during the withholding irrigation and after the withholding irrigation; vertical bars are standard deviations

Fig. 7 Relationships between transpiration in W m^{-2} and wind speed (u) for two specific meteorological conditions for both treatments, at hourly scale; all available values were binned (bin equal to 0.5 m s^{-1}) and the standard deviations are not indicated for clarity
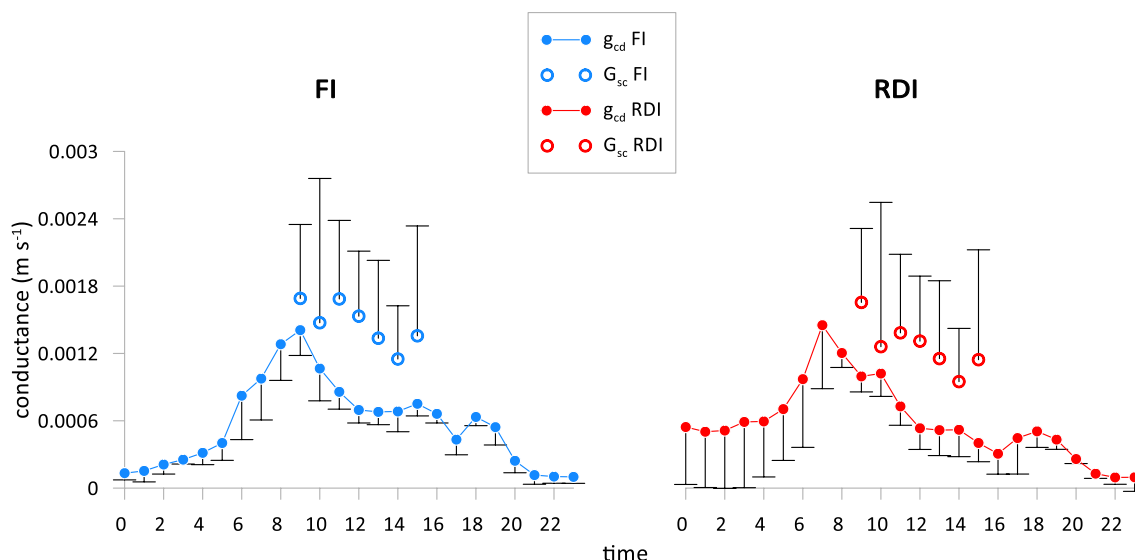
Fig. 8 Hourly patterns of canopy (g_{cd}) and stomatal (G_{sc}) conductances calculated as mean of all available values in 2019

the values are not significantly different, although the stomatal canopy conductances showed systematic higher values for both treatments, being 40 and 47% greater than diffuse canopy conductances for FI and RDI treatments, respectively. These differences are probably imputable to huge uncertainties due to the estimation of LAI from NDVI and to the physiological meaning of the two conductances. Furthermore, the canopy conductance hourly trend in Fig. 8 showed a typical asymmetrical pattern for this crop in both treatments (Fernández et al. 2006; Rodriguez-Dominguez et al. 2019), which can be explained by the combined effects of global radiation and VPD on stomatal regulation (Villalobos et al. 2000; Testi et al. 2006). In fact, canopy conductance rapidly increased from sunrise to its maximum value 3–5 h afterwards, and then decreased throughout the daytime period, with a rapid decline until early afternoon and a slower variation thereafter the lowest values just before night.

The absolute values and the daily patterns of g_{cd} and g_a (Fig. 6) address the absolute values and trends of the decoupling factor Ω (see Eq. 6), illustrated at hourly scale during daytime ($R_g > 20$ Wm^{-2}, hours 5:00–20:00) in Fig. 9, for all available data in the three irrigation periods and both treatments. Since g_a values are always much highest than g_{cd} values, Ω mainly follows the canopy conductance trends, with double peaks in the morning and in the afternoon, and minimum values in the hottest hours (Oguntunde 2005). Therefore, g_{cd} was the major factor in controlling energy partitioning during the whole growing season, as indicated by the very low Ω values, which ranged between 0.00 and 0.05.

Furthermore, although Ω was not significantly different in FI and RDI when considering all available night and day values, however during daytime it is significantly ($P<0.05$)

higher in RDI than in FI, exactly as for the canopy conductance during the withholding irrigation (Fig. 9b), being in mean equal to 0.028±0.003 and 0.021±0.004 ms^{-1}, respectively, considering all available data in the three seasons, in contrast with the results by Tognetti et al. (2009), who found in olive orchard that rainfed olive trees were more coupled to the atmosphere than those fully irrigated.

While the relation between Ω and canopy conductance is implicit in the calculation (see Eq. 6) and, moreover, was amply demonstrated for many crop types including trees (see de Kauwe et al. 2017 for a review), the relationship between other indicators of crop water status and the decoupling factor is contradictory. Spinelli et al. (2018) did not find any relationship between Ω and the stem water potential in almond trees, as well as Oguntunde (2005), who found that the decoupling factor did not respond to the soil water shortage in a Cassava crop. Nevertheless, apart the wind speed that has direct influence on Ω (Wullschleger et al. 2000; de Kauwe et al. 2017, among many others), the impact of environmental factors on decoupling factor can be analysed by the relationships between the precipitations and the thermodynamical state of the atmosphere and Ω values (Wullschleger et al. 2000; de Kauwe et al. 2017). In Fig. 10, the relationships between the seasonal mean of the decoupling factor and the cumulated rain (upper panel) are shown. We found significant relationships ($P < 0.05$) between the degree of coupling and precipitation for both treatments, online with the insights by De Kauwe et al. (2017); in the present case, these relationships are logarithmic, showing a plateau at high values of the rain.

Since the critical conductance can be considered a synthetic index of the thermodynamical state of atmosphere (Katerji and Rana 2011, among others),

Fig. 9 Hourly trends during the day of aerodynamic the decoupling factor Ω (unitless) together with the standard deviations, for Full Irrigated (FI) and Regulated Deficit Irrigation (RDI) treatments, before the withholding irrigation for RDI (a), during the withholding irrigation (b)and after the withholding irrigation (c)
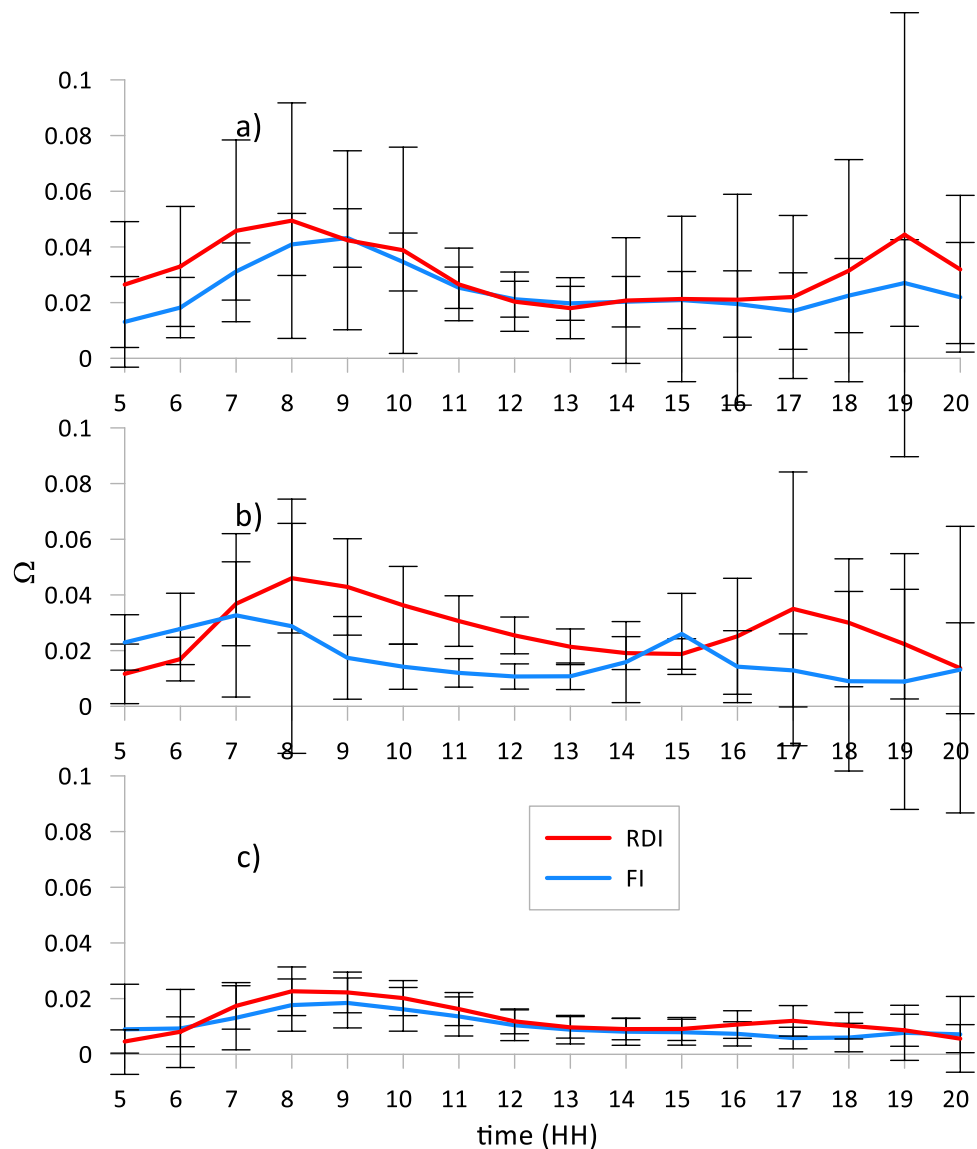
a relationship between decoupling factor and $g*$ was searched for; we found for both treatments a significant ($P<0.05$) linear relationship between Ω and $g*$ (Fig. 10, bottom panel). Both relations (Fig. 10 upper and bottom panels) showed higher year-to-year variability (lower r^2) for the full irrigated treatments (de Kauwe et al. 2017; Spinelli et al. 2018).

The hourly trend of Ω in the experimental period is illustrated in Fig. 11. It is generally low, but increasing after rain events, reaching value of 0.32–0.55 in the year 2019, 0.2–0.55 in the year 2020; it remains quite low (about 0.15) in the third year also after rain. This corresponds to very high values of canopy conductance just in the first hours after rain (data not shown in detail) when the plants have fully soil water, available energy become fully available, and all surfaces are saturated. In this case transpiration becomes increasingly dependent on the available energy and less

dependent on vapour pressure deficit (Wullschleger et al. 2000; Tognetti et al. 2009; De Kauwe et al. 2017).

This suggests a link between the decoupling factor and the structure resistance r_0, measurable only in these specific conditions of water saturation (see Appendix I). In fact, an estimation of r_0 in those conditions brings to a value of 68.8 ± 28.9 s m^{-1}, corresponding to a canopy conductance of 0.019 ± 0.013 m s^{-1}, comparable to the aerodynamic conductance values permitting a partial increasing of the equilibrium between the crop in given water conditions and the atmosphere.

4 Conclusions and recommendations

The hedge olive plantation studied is generally very well coupled to the atmosphere, regardless of soil water conditions; therefore, the transpiration is mainly

Fig. 10 Relationship between the decoupling factor (Ω) and cumulated rain (top panel) and critical conductance (g*) (bottom panel)
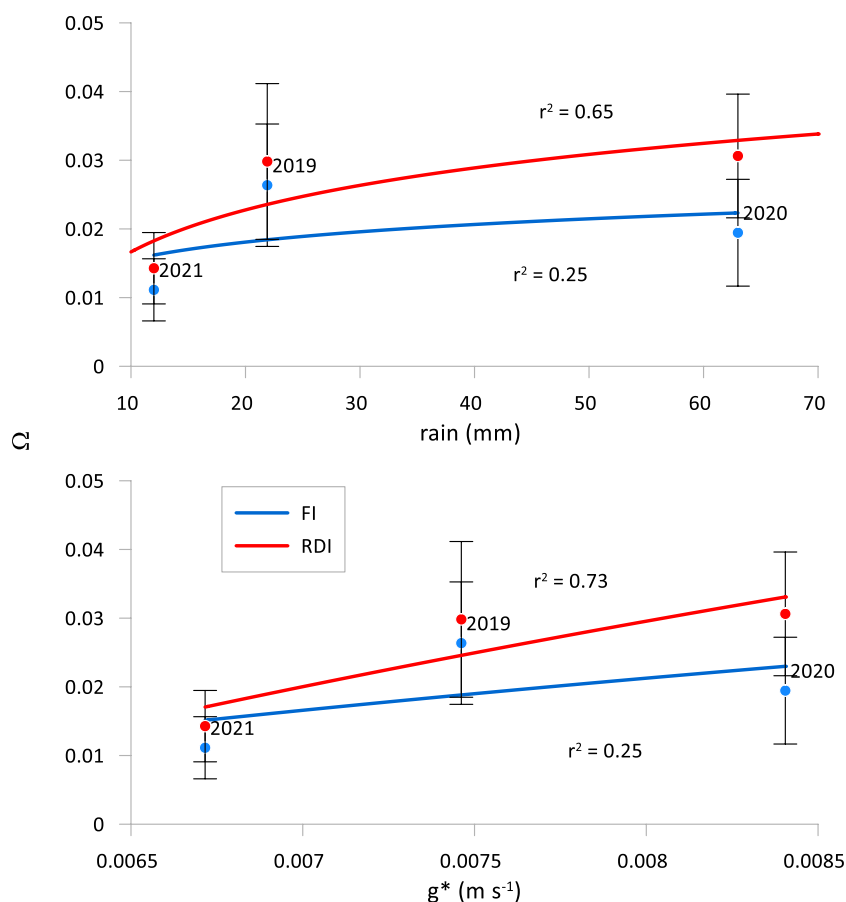
addressed by the canopy conductance. For this super high density olive orchard, the decoupling factor Ω is generally very low because the canopy conductance is much smaller than the aerodynamic conductance in any water and climatic conditions, except when all canopy surfaces are saturated in water.

The approximations introduced in this study (mainly the neglecting soil evaporation and the adoption of standard Granier's a and b coefficients in TDM instead of specie-specific values) do not affect the general conclusions, since the aerodynamic conductance determined in the investigated hedgerow olive orchard is always almost two orders greater than the estimated diffuse canopy conductance.

Apart the wind speed and the aerodynamical characteristics, which address the elasticity of the decoupling factor, furthermore, the plant water status has influence on Ω values, which are generally higher when the olive orchard is submitted to regulated deficit irrigation.

Furthermore, at seasonal scale, the coupling factor increase with the increasing of the precipitation regime, as well as the increase of the thermodynamical state of

atmosphere, as synthetized by the critical conductance expression (i.e. increasing of available energy and decreasing of the vapour pressure deficit).

After rain, in the brief periods when all surfaces are saturated, the canopy conductance increases its value due to the contribution to an "excess conductance" attributable to the structure of the transpiration surfaces. Hence, this canopy structure conductance increases the Ω values, by reducing the coupling of the canopy with the atmosphere.

Furthermore, from the experimental point of view, the following points should be considered when the decoupling process is studied for hedgerow tree canopies:

1. The roughness of the canopy depends on the wind direction and the orientation of the row and should be calculated accordingly, avoiding constant values of z_0 in the aerodynamic conductance calculation.
2. In the estimation of the aerodynamic conductance the wind speed should be determined above the crop or upscaled from the station to the crop if the measurement of the wind speed is carried out far from the canopy.

Fig. 11 Hourly trend of the decoupling factor Ω in the experimental periods for both Full Irrigated (FI) and Regulated Deficit Irrigation (RDI) treatments, the precipitations are also illustrated
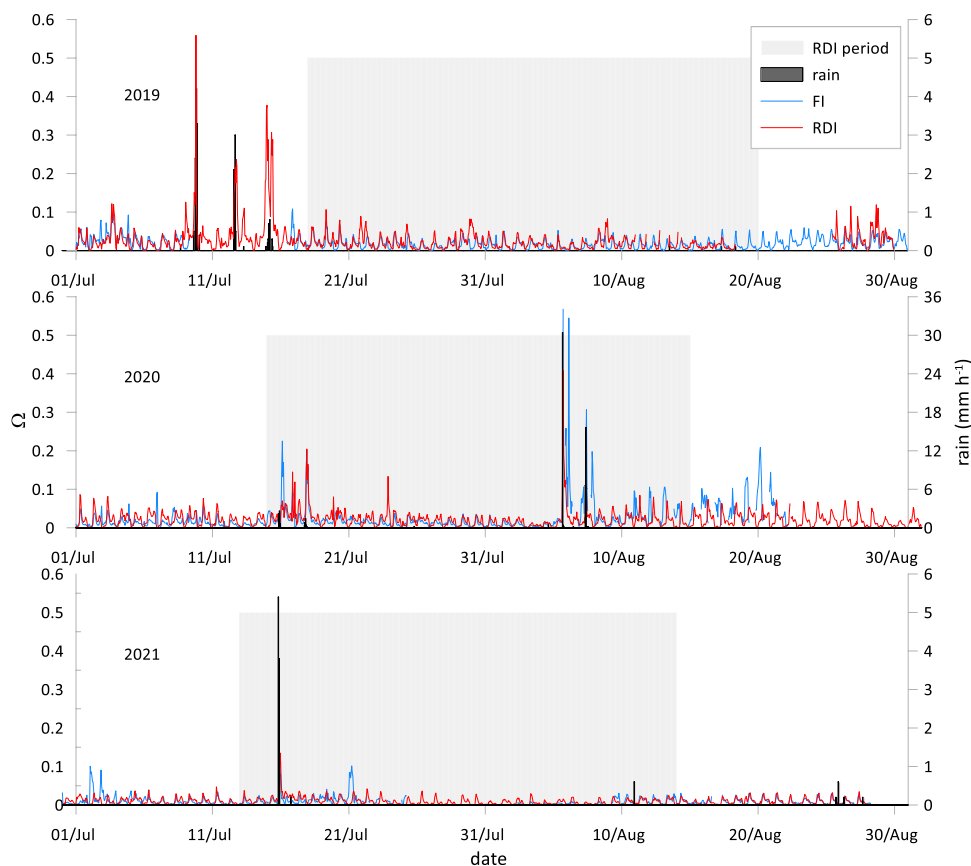
Appendix I

The potential crop evaporation E_p is defined (Katerji and Rana 2011, among many others) as the evaporation of a crop having all evaporative surfaces (leaves, stems, soil) saturated or covered in water. Thus (Eq. 1), no biological control is exerted for the water losses (the crop stomatal conductance $G_s \rightarrow \infty$, as well as g_c):

$$\lambda E_p = \frac{\varepsilon A + \rho c_p D g_a / \gamma}{\varepsilon + 1} \tag{I.1}$$

Yet, the crop itself shows a resistance to water vapour transfer, r_0, due to its structure (Perrier 1975a, 1975b; Rana et al. 1994; Daudet et al. 1999; Katerji and Rana 2011). Even if this variable could be thought as a theoretical concept, however it has practical impacts, and it is found in nature, although only during relatively short periods, when free water evaporates from leaves just after a rain, a strong dew or an accurate irrigation by aspersion. Under these conditions it is possible to determine the resistance r_0; in fact, in this case the canopy conductance to the diffusion of water vapour can be written as:

$$\frac{1}{g_{cd}} = r_0 + r_{min} \tag{I.2}$$

where r_{min} is the minimum canopy resistance of the "big leaf" to the maximum potential transpiration. Combining Eqs. (1), (I.1) and (I.2), the expression of the structure resistance become:

$$r_0 = \frac{\varepsilon + 1}{g_a} \left(\frac{\lambda E_p}{\lambda T} - 1 \right) - r_{min} \tag{I.3}$$

here r_{min} is set equal to 67.9 s m^{-1} (Villalobos et al. 2000).

Data availability Data are available under request to the authors. Pictures and description of used equipment are available under request.

Declarations

Ethics approval/declarations Not applicable

Consent to participate The authors, Gianfranco Rana, Gabriele De Carolis, Liliana Gaeta, Sergio Ruggeri, Rossana M. Ferrara, declare their consent to participate to the research on the hedgerow olive orchard in Mediterranean region.

Consent for publication The authors, Gianfranco Rana, Gabriele De Carolis, Liliana Gaeta, Sergio Ruggeri, Rossana M. Ferrara, declare their consent to publish the study: "Decoupling factor, aerodynamic and canopy conductances of a hedgerow olive orchard under Mediterranean climate".

Conflict of interest The authors declare no competing interests.

References

Alfieri JG, Kustas WP, Nieto H et al (2019) Influence of wind direction on the surface roughness of vineyards. Irrig Sci 37:359–373. https://doi.org/10.1007/s00271-018-0610-z

Baldocchi DD, Luxmoore RJ, Hatfield JL (1991) Discerning the forest from the trees: an essay on scaling canopy stomatal conductance. Agric For Meteorol 54:197–226. https://doi.org/10.1016/0168-1923(91)90006-C

Bonachela S, Orgaz F, Villalobos FJ, Fereres E (2001) Soil evaporation from drip-irrigated olive orchards. Irrig Sci 20:65–71. https://doi.org/10.1007/s002710000030

Bréda N, Granier A, Barataud F, Moyne C (1995) Soil water dynamics in an oak stand. Plant Soil 172:17–27. https://doi.org/10.1007/BF00020856

Brito C, Dinis L-T, Ferreira H et al (2018) The role of nighttime water balance on Olea europaea plants subjected to contrasting water regimes. J Plant Physiol 226:56–63. https://doi.org/10.1016/j.jplph.2018.04.004

Campi P, Gaeta L, Mastrorilli M, Losciale P (2020) Innovative Soil Management and Micro-Climate Modulation for Saving Water in Peach Orchards. Front Plant Sci 11. https://doi.org/10.3389/fpls.2020.01052

Campi P, Mastrorilli M, Stellacci AM et al (2019) Increasing the effective use of water in green asparagus through deficit irrigation strategies. Agric Water Manag 217:119–130. https://doi.org/10.1016/j.agwat.2019.02.039

Camposeo S, Godini A (2010) Preliminary observations about the performance of 13 varieties according to the super high density olive culture training system in Apulia (southern Italy). Adv Hortic Sci 24:16–20

Chebbi W, Boulet G, le Dantec V et al (2018) Analysis of evapotranspiration components of a rainfed olive orchard during three contrasting years in a semi-arid climate. Agric For Meteorol 256–257:159–178. https://doi.org/10.1016/j.agrformet.2018.02.020

Daudet FA, le Roux X, Sinoquet H, Adam B (1999) Wind speed and leaf boundary layer conductance variation within tree crown.

Agric For Meteorol 97:171–185. https://doi.org/10.1016/S0168-1923(99)00079-9

Daudet FA, Perrier A (1968) Etude de l'evaporation ou de la condensation a la surface d'un corps, a partir du bilan energetique

de Kauwe MG, Medlyn BE, Knauer J, Williams CA (2017) Ideas and perspectives: how coupled is the vegetation to the boundary layer? Biogeosciences 14:4435–4453. https://doi.org/10.5194/bg-14-4435-2017

Egea G, Diaz-Espejo A, Fernández JE (2016) Soil moisture dynamics in a hedgerow olive orchard under well-watered and deficit irrigation regimes: Assessment, prediction and scenario analysis. Agric Water Manag 164:197–211. https://doi.org/10.1016/j.agwat.2015.10.034

Fernández J-E (2014) Understanding olive adaptation to abiotic stresses as a tool to increase crop performance. Environ Exp Bot 103:158–179. https://doi.org/10.1016/j.envexpbot.2013.12.003

Fernández JE, Díaz-Espejo A, Infante JM et al (2006) Water relations and gas exchange in olive trees under regulated deficit irrigation and partial rootzone drying. Plant and Soil 284:273–291. https://doi.org/10.1007/s11104-006-0045-9

Fernández JE, Moreno F, Girón IF, Blázquez OM (1997) Stomatal control of water use in olive tree leaves. Plant and Soil 190:179–192. https://doi.org/10.1023/A:1004293026973

Fernández JE, Perez-Martin A, Torres-Ruiz JM et al (2013) A regulated deficit irrigation strategy for hedgerow olive orchards with high plant density. Plant and Soil 372:279–295

Forster MA, Kim TDH, Kunz S et al (2022) Phenology and canopy conductance limit the accuracy of 20 evapotranspiration models in predicting transpiration. Agric For Meteorol 315:108824. https://doi.org/10.1016/j.agrformet.2022.108824

Godini A, Vivaldi GA, Camposeo S (2011) Olive cultivars field-tested in super-high-density system in southern Italy. Calif Agric (Berkeley) 65:39–40. https://doi.org/10.3733/ca.v065n01p39

Granier A (1985) Une nouvelle methode pur la mesure du flux de seve brute dans le tronc des arbres (A new method of sap flow mensurement in tree stems). Annales des Sciences Forestières 42(2): 193–200 (in French)

Granier A (1987) Evaluation of transpiration in a Douglas-fir stand by means of sap flow measurements. Tree Physiol 3:309–320. https://doi.org/10.1093/treephys/3.4.309

Grossiord C, Forner A, Gessler A et al (2015) Influence of species interactions on transpiration of Mediterranean tree species during a summer drought. Eur J For Res 134:365–376. https://doi.org/10.1007/s10342-014-0857-8

Iniesta F, Testi L, Orgaz F, Villalobos FJ (2009) The effects of regulated and continuous deficit irrigation on the water use, growth and yield of olive trees. Eur J Agron 30:258–265. https://doi.org/10.1016/j.eja.2008.12.004

Jarvis PG, McNaughton KG (1986) Stomatal Control of Transpiration: Scaling Up from Leaf to Region. pp 1–49

Katerji N, Rana G (2011) Crop Reference Evapotranspiration: A Discussion of the Concept, Analysis of the Process and Validation. Water Resources Management 25:1581–1600. https://doi.org/10.1007/s11269-010-9762-1

Katerji N, Rana G, Ferrara RM (2017) Actual evapotranspiration for a reference crop within measured and future changing climate periods in the Mediterranean region. Theor Appl Climatol 129:923–938. https://doi.org/10.1007/s00704-016-1826-6

Kjelgaard JF, Stockle CO (2001) Evaluating surface resistance for estimating corn and potato evapotranspiration with the Penman–Monteith model. Transactions of the ASAE 44:797

Köstner BMM, Schulze E-D, Kelliher FM et al (1992) Transpiration and canopy conductance in a pristine broad-leaved forest of Nothofagus: an analysis of xylem sap flow and eddy correlation measurements. Oecologia 91:350–359. https://doi.org/10.1007/BF00317623

Lee X, Massman W, Law B (Eds.) (2004) Handbook of micrometeorology: a guide for surface flux measurement and analysis (Vol. 29). Springer Science & Business Media

Lopez-Bernal A, Alcantara E, Testi L, Villalobos FJ (2010) Spatial sap flow and xylem anatomical characteristics in olive trees under different irrigation regimes. Tree Physiol 30:1536–1544. https://doi.org/10.1093/treephys/tpq095

Marin FR, Angelocci LR, Nassif DSP et al (2016) Crop coefficient changes with reference evapotranspiration for highly canopy-atmosphere coupled crops. Agric Water Manag 163:139–145

Martin P (1989) The significance of radiative coupling between vegetation and the atmosphere. Agric For Meteorol 49:45–53

Maurer KD, Bohrer G, Kenny WT, Ivanov VY (2015) Large-eddy simulations of surface roughness parameter sensitivity to canopy-structure characteristics. Biogeosciences 12:2533–2548

Maurer KD, Hardiman BS, Vogel CS, Bohrer G (2013) Canopy-structure effects on surface roughness parameters: Observations in a Great Lakes mixed-deciduous forest. Agric For Meteorol 177:24–34

McNaughton KG, Jarvis PG (1991) Effects of spatial scale on stomatal control of transpiration. Agric For Meteorol 54:279–302

McNaughton KG, Jarvis PG (1983) Predicting effects of vegetation changes on transpiration and evaporation. Water deficits and plant growth 7:1–47

Monteith JL, Unsworth MH (1990) Principles of En-vironmental Physics. 2nd edn Edward Arnold, London pp. 291

Monteith JL (1986) How do crops manipulate water supply and demand? Philos Trans Royal Soc A PHILOS T R SOC A 316:245–259

Monteith JL (1965) Evaporation and environment. In: Symposia of the society for experimental biology. Cambridge University Press (CUP), Cambridge, pp 205–234

Naresh Kumar M, Murthy CS, Sesha Sai MVR, Roy PS (2009) On the use of Standardized Precipitation Index (SPI) for drought intensity assessment. Meteorol Appl 16:381–389. https://doi.org/10.1002/met.136

Oguntunde PG (2005) Whole-Plant Water use and Canopy Conductance of Cassava Under Iimited Available Soil Water and Varying Evaporative Demand. Plant Soil 278:371–383. https://doi.org/10.1007/s11104-005-0375-z

Perrier A (1975a) Etude physique de l'évapotranspiration dans les conditions naturelles. I. Evaporation et bilan d'énergie des surfaces naturelles (Phyisics of evapotranspiration in natural conditions. I. evaporation and energy balance in natural surfaces). Annales Agrononomiques 26:1–18 (In French)

Perrier A (1975b) Etude physique de l'évapotranspiration dans les conditions naturelles. III. Evapotranspiration réelle et potentielle des couverts végétaux (Phyisics of evapotranspiration in natural conditions. III. Actual and potential evapotranspiration in vegnattated surfaces). Annales Agronomiques 26:229–243 (In French)

Priestley CHB, Taylor RJ (1972) On the assessment of surface heat flux and evaporation using large-scale parameters. Mon Weather Rev 100:81–92

Rana G, Katerji N (2009) Operational model for direct determination of evapotranspiration for well watered crops in Mediterranean region. Theor Appl Climatol 97:243–253

Rana G, Katerji N, Mastrorilli M (1997) Environmental and soil-plant parameters for modelling actual crop evapotranspiration under water stress conditions. Ecol Model 101:363–371

Rana G, Katerji N, Mastrorilli M, el Moujabber M (1994) Evapotranspiration and canopy resistance of grass in a Mediterranean region. Theor Appl Climatol 50:61–71

Rana G, Muschitiello C, Ferrara RM (2016) Analysis of a precipitation time series at monthly scale recorded in Molfetta (south Italy) in the XVIII century (1784-1803) and comparisons with present pluviometric regime. Italian Journal of Agrometeorology 3:23–30

Resco de Dios V, Chowdhury FI, Granda E et al (2019) Assessing the potential functions of nocturnal stomatal conductance in C3 and C4 plants. New Phytol 223:1696–1706

Rochette P, Pattey E, Desjardins RL et al (1991) Estimation of maize (Zea mays L.) canopy conductance by scaling up leaf stomatal conductance. Agric For Meteorol 54:241–261

Rodriguez-Dominguez CM, Hernandez-Santana V, Buckley TN et al (2019) Sensitivity of olive leaf turgor to air vapour pressure deficit correlates with diurnal maximum stomatal conductance. Agric For Meteorol 272:156–165

Rosecrance RC, Krueger WH, Milliron L et al (2015) Moderate regulated deficit irrigation can increase olive oil yields and decrease tree growth in super high density 'Arbequina'olive orchards. Sci Hortic 190:75–82

Spinelli GM, Snyder RL, Sanden BL et al (2018) Low and variable atmospheric coupling in irrigated Almond (Prunus dulcis) canopies indicates a limited influence of stomata on orchard evapotranspiration. Agric Water Manag 196:57–65

Szeicz G, Long IF (1969) Surface resistance of crop canopies. Water Resour Res 5:622–633

Testi L, Orgaz F, Villalobos FJ (2006) Variations in bulk canopy conductance of an irrigated olive (Olea europaea L.) orchard. Environ Exp Bot 55:15–28

Tognetti R, Giovannelli A, Lavini A et al (2009) Assessing environmental controls over conductances through the soil–plant–atmosphere continuum in an experimental olive tree plantation of southern Italy. Agric For Meteorol 149:1229–1243. https://doi.org/10.1016/j.agrformet.2009.02.008

Villalobos FJ, Orgaz F, Testi L, Fereres E (2000) Measurement and modeling of evapotranspiration of olive (Olea europaea L.) orchards. Eur J Agron 13:155–163

Vivaldi GA, Strippoli G, Pascuzzi S et al (2015) Olive genotypes cultivated in an adult high-density orchard respond differently to canopy restraining by mechanical and manual pruning. Sci Hortic 192:391–399

Wullschleger SD, Wilson KB, Hanson PJ (2000) Environmental control of whole-plant transpiration, canopy conductance and estimates of the decoupling coefficient for large red maple trees. Agric For Meteorol 104:157–168

Zeng X, Wang A (2007) Consistent parameterization of roughness length and displacement height for sparse and dense canopies in land models. J Hydrometeorol 8:730–737

Zhang ZZ, Zhao P, McCarthy HR et al (2016) Influence of the decoupling degree on the estimation of canopy stomatal conductance for two broadleaf tree species. Agric For Meteorol 221:230–241